Tanzania Journal of Engineering and Technology 2023, **42**(**3**):154-170
OPEN ACCESS articles distributed under Creative Commons
Attribution Licence [CC BY-ND]
Websites: https://ajol.org/tjet; https://tjet.udsm.ac.tz

ISSN 1821-536X (**print**); ISSN 2619-8789 (**electronic**)
https://doi.org/10.52339/tjet.v42i3.963

Regular Research Manuscript

Designing a Model of Solar Photovoltaic Water Pumping System for Off-Grid Localities in Tanzania

Imani S. Mruma[1,2†] and Sarah P. Ayeng'o[2]

[1]Department of Mechanical and Industrial Engineering, College of Engineering and Technology, University of Dar es Salaam, P.O. Box 35131, Dar es Salaam, Tanzania
Ministry of Energy (MoE), Government of United Republic of Tanzania, P.O. Box 2494, 40488 Dodom, Tanzania
[†]Corresponding author: imanisteve@gmail.com
[†]ORCID: https://orcid.org/0009-0002-1799-3806

ABSTRACT

Modeling of photovoltaic (PV) water pumping system for rural water localities is vital especially in these modern days, in Tanzania. This is due to the rise of high number of solar-powered rural water projects constructed lacking appropriate design. The fate result into poor and substandard projects delivering below expectations. Kikombo Solar Water Project situated in Dodoma; Tanzania is one among poorly designed solar project chosen as a case study to validate proposed model. The main problem of Kikombo project is unsatisfactory amount of water from domestic points to satisfy population demand. This matter has been raised by pumping-station attendants and the Kikombo village community. The Kikombo water project can only deliver 14.21 m^3/day while required demand is 50 m^3/day. In order to solve the existing problem, solar water pumping model was developed. It consists of PV array, a motor-pump (AC), inverters (DC–AC converter), maximum power point tracker (MPPT) integrated with a controller and a storage water tank. Analysis was done in MATLAB to estimate which parameters should be upgraded to meet the water requirements. Moreover, the input and output variable for each model component were identified and simulated in MATLAB software. Finally, PV model was validated and system capacity improvement to rectify designs limitation for Kikombo is proposed. The model results were validated through real measurement data at Kikombo water pumping station. The differential error of 0.04062 was observed as a system error. PV model displayed an error of 0.0509 for power output, 0.0383 for current and 0.0131 for voltage; inverter displayed error of 0.0686 and 0.0406 for motor pump. In order to acquire sufficient water demand of 50 m^3 /day, the PV panel and pump capacities should be increased to 8.82 kW and 7.35 kW respectively from the existing PV panel's power of 2.5 kW and motor-pump of 4 kW.

ARTICLE INFO
Submitted: **June, 2022**
Revised: **Feb., 2023**
Accepted: **Jul. 15, 2023**
Published: **Oct., 2023**

Keywords: *Solar power, PV pumping system, PV cell and array, Inverter, Motor pump.*

INTRODUCTION

The main energy source for extracting water in rural areas is human physical strength, through hand pumps or with buckets in wells (World_Bank, 2020). Such collection techniques are time consuming, very physically demanding and prevent from reaching deep aquifers. Using electrified solutions from non-renewable or renewable sources has been attempted. In general, the non-renewable solutions are based on diesel, but water pumping systems powered by photovoltaic energy have been expanding.

The solar-powered pumping system can be appropriate for rural areas which are facing energy crisis. Due to geographical position, Tanzania has plenty of sunshine through the year which makes it ideal location for utilization of solar energy. Small farms, villages, and animal herds in developing countries require hydraulic output power of less than a kilowatt.

Surprisingly, the degree of acceptance of photovoltaic solar water pumping systems by the users is still very low. There are several factors, which have inhibited the widespread implementation of these systems. These include the high initial cost; lack of awareness and technical expertise; lack of sufficient knowledge on the daily output of these systems; and a history of failures (AfDB_Group, 2015; Bishoge et al., 2018). For example, several solar water-pumping systems are installed in various areas in Tanzania, but most of these systems have experienced problems, mainly because they were not properly sized (Juma et al., 2021). The output in terms of the daily volume of water pumped was reported below the expectation of the users.

Solar water pumping systems have wider advantages such as an abundant renewable energy, a non-polluting technology which does not release greenhouse gases. In addition, they have the subsidy of storing water for use when the sun is not shining, eliminating the need for battery. This simplifies the design and reduces the overall system costs. Other technical benefit includes: noiseless technology as there are few moving parts involved in energy generation (Bishoge et al., 2018). This technology requires low-maintenance because of lack of moving parts. It can be installed on modular basis and expenditure over a period of time. Solar-powered systems are often considered for use in developing countries instead of other forms of alternative energy because they are durable and exhibit long-term economic benefits (Aliyu et al., 2018).

MATERIAL AND METHODS

Description of the Study Area

Kikombo solar water project is located in Dodoma region, Tanzania. The region is classified as semi-arid area and has a great potential in solar radiation. Its approximated potential solar energy is 1800–1900 kWh/kWp per year (Ayeng'o, 2019). The Kikombo site is situated 21 km from the Dodoma city centre. The project was constructed in 2015 to provide water service to the community of about 2,300 populations. Technology option was borehole using a PV powered system comprising of 17 water points and storage tanks of 50 m^3, pumping head of 187 m, borehole depth of 150 m, abstraction depth of 140 m and borehole yield capacity 11.5 m^3/hr. Installed capacities of each component is shown in Table 1.

Table 1: Kikombo solar water project installed components technical data

No.	ITEM	SPECIFICATION
1	Community population	~2,300
2	Tank capacity	50 m^3
3	Water/domestic points (DPs)	17
4	Pumping head	187 m
5	Power source	3-phase system from solar PV
Borehole data		

No.	ITEM	SPECIFICATION
1	Borehole yield capacity	11.5 m^3/hr
2	Well depth	150 m
3	Abstraction depth	140 m
Motor-Pump (submersible pump)		
1	Flow rate (capacity)	7.0 m^3/hr
2	Pumping head	140 m
3	Motor power	4.0 kW
Solar PV Module		
1	Rated power (P_{mp})	315 W
2	Voltage at maximum power (V_{mp})	38.44 V
3	Current at maximum power (I_{mp})	8.20 A
4	Open circuit voltage (V_{oc})	45.75 V
5	Short circuit current (I_{sc})	8.72 A
6	Total number of cells in series (N_s)	76
7	Total number of cells in parallel (N_p)	1
Inverter specification		
1	Maximum DC input voltage	375 V
2	Rated power	4.0 kW
3	Rated voltage (AC_{out})	60 – 240 V
4	Maximum input/output current	14 A
5	Efficiency	85%
6	Frequency	50/60 Hz

Figure 1 shows some of the photos taken at Kikombo solar water pumping station. The photos show how the water pumping project was installed.

Figure 1: Physical picture for Kikombo water pumping project.

A stand-alone photovoltaic water pumping system (PVWPS) consists of a PV array, a motor-pump (AC), hydraulic system, inverters (DC–AC converter), power controllers, charge regulator, maximum power point tracker integrated with a controller and a storage unit which can be either a water tank or batteries. These components should be chosen well-matched according to their electrical properties.

The Kikombo water project uses submersible pump (centrifugal type) which are simple, low cost and available for a wide range of flow rates and heads. These pumps have relatively high efficiency at high head and are the most commonly employed pumps in rural regions because of their good performance curves with accuracy (Malla et al., 2011). Induction motors (AC) are installed in line with submersible pumps as they are cheap, long-life span, high speed and power compared to DC motors. They also require less maintenance due to absence of commutators, slip rings and brushes on their configuration (Benghanem et al., 2013; Aliyu et al., 2018).

Although using batteries in a system will maximize the pump efficiency because of the steady operating conditions presented to the pump and motor, but no battery application will be considered as they increase project cost. The use of storage batteries becomes costly in the short and long term (Marcel et al., 2021). It is usually less expensive to store water than to store electricity. Architecture of the photovoltaic water pumping system considered is presented in Figure 2 (Malla et al., 2011; Aliyu et al., 2018).

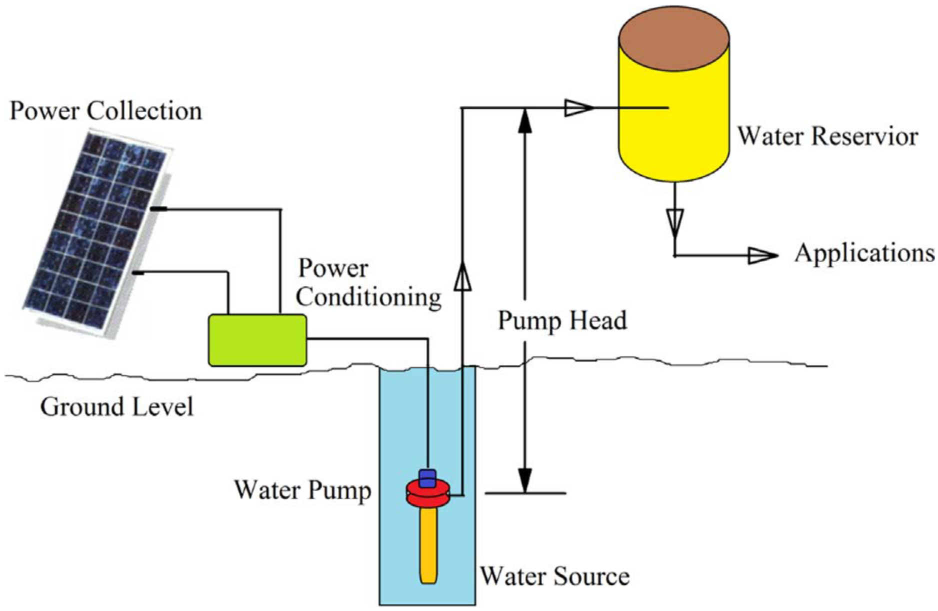

Figure 2: Schematic diagram of a solar powered water pumping system.

Model Input Data

The developed model consisted of the following main input parameters: solar radiation, temperature, inclination angle, latitude angle, pumping head and water demand (Figure 3). Global solar radiation and diffuse radiation are usually measured using pyrometer, while direct radiation is measured using pyrheliometer. Reflected radiation is determined by subtracting the measured direct and diffuse radiation from the global solar radiation (Chilundo et al., 2018; Justo and Mushi, 2020). Thermometer is usually used to measure ambient temperature. Figure 4 represents the global, direct, diffuse solar radiation and temperature for Dodoma region. Latitude angle of 6.1630˚S and 15° inclination angle were used in the model.

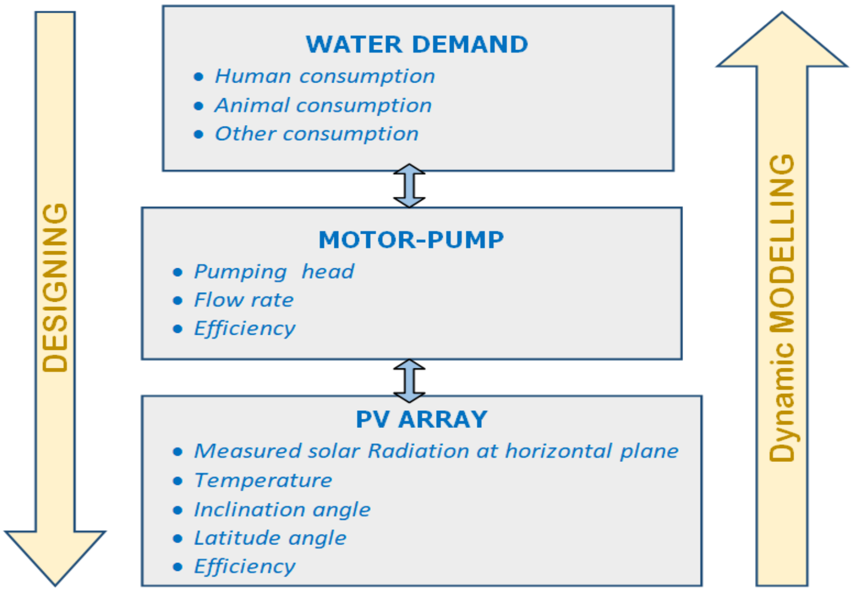

Figure 3: Solar water pumping systems model input parameters (Elia et al., 2013).

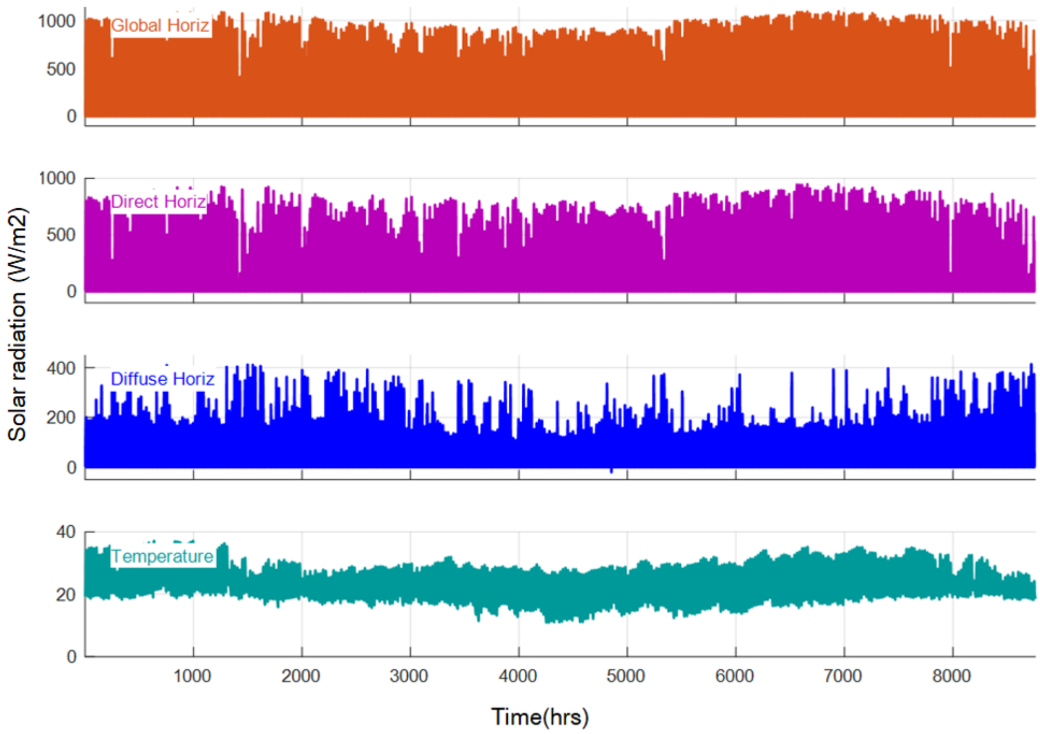

Figure 4: Horizontal global, direct, diffuse solar radiation and temperature data for Dodoma.

Total Dynamic Head

In solar water pumping system, the appropriate pump is selected depending on the water requirement and duty head for lifting water (Bolaji et al., 2007).

According to the specific application, pump size selection depends upon water demand per day, elevation head and operational cost.

Total dynamic head is the pump duty head for lifting water from pump-set (pump position level inside borehole) to tank level (tank inlet pipe) including all possible pipe frictional losses. Static head is a difference in height between ground level (surface) and static water level. While pumping, water level drops forming the drawdown, which is the difference in height between static water level and drawdown level. At last, total dynamic head is the summation of tank elevation head to ground level as Figure 5 shows. Kikombo solar water project has a total dynamic head of 187 m which was also considered in the model.

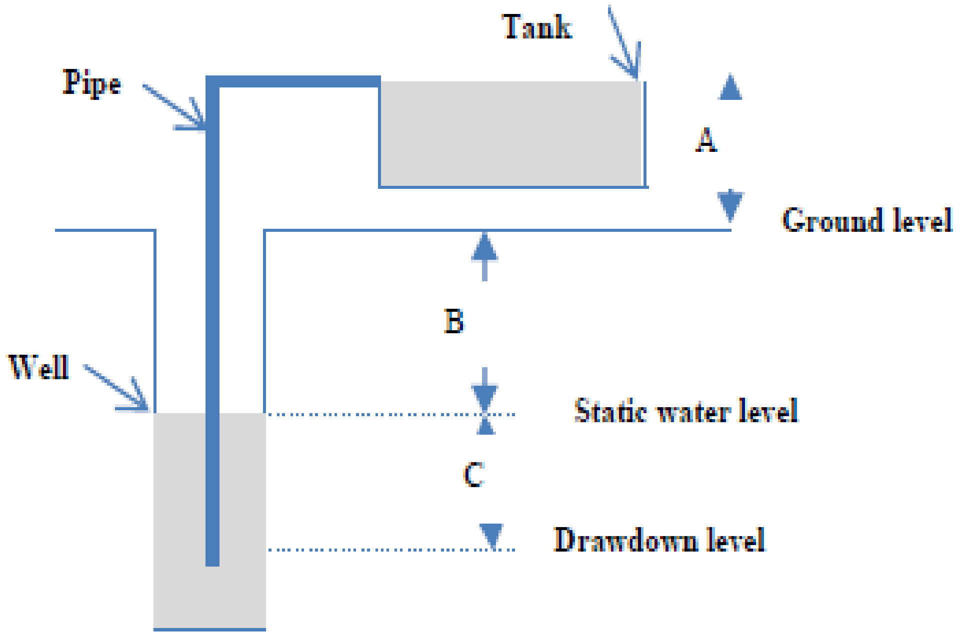

Figure 5: Typical head of the water pump.

Total water requirement includes all consumption from human, animal, hospital, schools, offices etc. Water demand is calculated as total water consumption demand of the inhabitants (m³/day) including other water activities requirements. The following formula is used,

$$Q = Q_{hc} + Q_{ac} + Q_{oc} \tag{1}$$

where, Q is the total water demand per day (m³/day), Q_{hc} is the daily water demand for human consumption, Q_{ac} is the daily water demand for animal consumption and Q_{oc} is the daily water demand for other consumption of institutions (e.g., hospital/dispensary, and schools/offices).

Photovoltaic Array Model

Photovoltaic array is modeled by considering horizontal solar radiation, temperature, inclination, latitude angles and PV panel characteristics as its input data. PV array is usually designed primarily from PV cell model. Here is where all the inputs are fed to attain cell output current and voltage, which both then gives PV cell power. Table 2 describes the used solar PV module characteristics.

Table 2: PV characteristics data of the module used

	Monocrystalline photovoltaic module parameter (IF-P315-72 IFRI-SOL)	
	Name	**Values**
1	Open circuit voltage (V_{oc})	45.75 V
2	Short circuit current (I_{sc})	8.72 A
3	Number of Cell connected in Series (N_s)	76
4	Number of cells connected in parallel (N_p)	1
5	Temperature coefficient of short circuit current (k_i)	0.1020%
6	Temperature coefficient of open circuit voltage (T_{C_Voc})	-0.3610%
7	Values at standard test conditions (irradiance, temperature & air mass, wind)	1000 W/m^2; 25 °C; 1.5; 1 m/s)
8	*NOCT*	46°C
9	Series resistance (R_s)	0.1884 Ω
10	Shunt resistance (R_{sh})	299.99 Ω
11	Diode ideality factor (n)	0.9476
12	Electron charge (q)	1.6×10^{-19}
13	Boltzman constant (K)	1.38×10^{-23}
14	Band energy gap of semiconductor (E_g)	$1.1 \text{ eV} = 1.1 \times 1.6 \times 10^{-19} = 1.76 \times 10^{-19}$

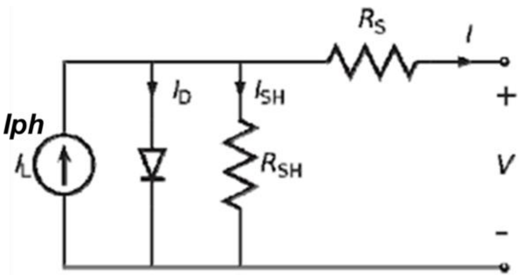

Figure 6: Solar cell equivalent circuit.

A solar cell is usually represented by an electrical equivalent circuit of current source and diode as in Figure 6. The following are formulas that were used to calculate output current (I) generated by the PV cell using from Kirchhoff's law (Bolaji et al., 2007; Ayeng'o, 2019; Minja and Mushi, 2023).

$$I = I_{pv} = I_{ph} - I_d - I_{sh} \tag{2}$$

where I_{ph} is photo-current, I_d is diode current. Resistance in parallel is termed shunt resistance *(R_{sh})*. The photocurrent which depends on irradiance G and temperature T given by Equation (3) as expressed by Fungo et al. (2021).

$$I_{ph} = \left[I_{SC} + k_i\left(T - 298\right)\right]\frac{G}{G_0} \tag{3}$$

The shunt resistance current given as $I_{sh} = (V+IR_s)/R_{sh}$ gives the output current from PV cell output by the Equation (4).

$$I = I_{ph} - I_0\left(\exp\left(\frac{V + IR_s}{nKN_sT}\right) - 1\right) - I_{sh} \tag{4}$$

where V is the cell output voltage (given as module voltage divided by N_s), I_{sh} is the shunt current, q refers to the charge of the electron (equal to 1.6 x 10^{-19} C), I_o is the dark saturation current, K refers to the Boltzmann's constant (equal to 1.38x10^{-23} J/K), T is the operating cell temperature in Kelvin (K), N_s refer to number of cells connected in series, R_s is the series resistance.

Calculation for maximum voltage (V_{max}), current (I_{max}) and power (P_{max}) are as derived in Equations (5) – (7) opted from (Masters, 2013).

$$\exp\left(\frac{eV_{\max}}{kT_C}\right)\left(1 + \frac{eV_{\max}}{kT_C}\right) = 1 + \frac{I_{SC}}{I_0} \tag{5}$$

$$I_{\max} = \left(\frac{eV_{\max}}{kT_C + eV_{\max}} \right) \left(I_{SC} + I_0 \right) \quad (6)$$

$$P_{\max} = V_{\max} I_{\max} \quad (7)$$

Solving the V_{max} (5), a nonlinear equation is complex, therefore MATLAB program is used to get solutions in a very short time. The Equation (8) is used to get temperature of the solar cell (Sarhan et al., 2006; Tian et al., 2012).

$$T_C = T_{air} + \frac{NOCT - 20}{80} H_t \quad (8)$$

Where T_c is the temperature of solar cell (˚C), T_{air} is the ambient/air temperature (˚C), *NOCT* is the nominal operating cell temperature (˚C) at ambient temperature of 20˚C, H_t is the irradiance measured at inclined plane (mW/cm^2). To get output voltage of a PV module, Equation (9) is employed (Moharram, 2013; Karafil, 2016).

$$V = V_{\max} \left(1 + \left(TC_{VOC\%} \left(T_{Op-c} - T_{STC} \right) \right) \right) \quad (9)$$

Where $T_{op\text{-}c}=(NOCT\text{-}20)$ is the operating cell temperature; T_{STC} is the temperature at standard test condition (25˚C); T_{air} is the ambient/air temperature (˚C); $TC_{VOC\%}$ is the temperature coefficient of open circuit voltage. Global solar radiation at an inclined plane (H_t) is obtained as a summation of direct/beam (H_b), diffuse (H_d), and reflected (H_r) solar radiation at inclined plane (Ayeng'o, 2019) in Equation (10).

$$H_t = H_b + H_d + H_r \quad (10)$$

From above expressions, supportive formulas to be employed are described in following equations. Direct solar radiation at inclined plane is given by Equation (11),

$$H_b = H_{b,0} \cos(z) \quad (11)$$

where, $H_{b,0}$ is the the beam solar radiation measured at horizontal plane (W/m^2); z is the solar Zenith angle, which is the angle between the inclined and the vertical planes. Diffuse solar radiation at inclined plane is computed by Equation (12).

$$H_d = \frac{1}{2} \left(1 + \cos(\beta) \right) H_{d,0} \quad (12)$$

Where $H_{d,0}$ is the diffuse solar radiation measured at horizontal plane (W/m^2); and β is the inclination (tilt) angle (°). Reflected solar radiation at inclined plane is captured by Equation (13),

$$H_r = \frac{1}{2} \left(1 + \cos(\beta) \right) H_{t,0} \alpha_s \quad (13)$$

where, $H_{t,0}$ is the global solar radiation at horizontal plane and α_s is the ground reflectivity (also known as albedo). Solar Zenith angle is computed by Equation (14).

$$\cos z = \cos\theta \cos\delta \cos h + \sin\theta \sin\delta \quad (14)$$

Where θ is the latitude angle; δ is the declination angle; h is the hour angle. Declination angle is computed by Equation (15); hour angle by Equation (16); and solar azimuth/albedo by Equation (17).

$$\delta = 23.45° \sin\left(\left(\frac{N - 80}{370} \right) 360 \right) \quad (15)$$

$$h = \frac{360}{24} T_t \quad (16)$$

$$\sin \alpha_s = \frac{\cos\delta \sin h}{\cos z} \quad (17)$$

Where N is the actual number of the day in a year (i.e., day 1, 2, 3...365). T_t is the time in 24-hour mode.

Figure 7 shows step by step the calculations involved on deriving the output power of a photovoltaic array. The simulation block representation of PV array model in MATLAB with input and output data is as shown in Figure 8.

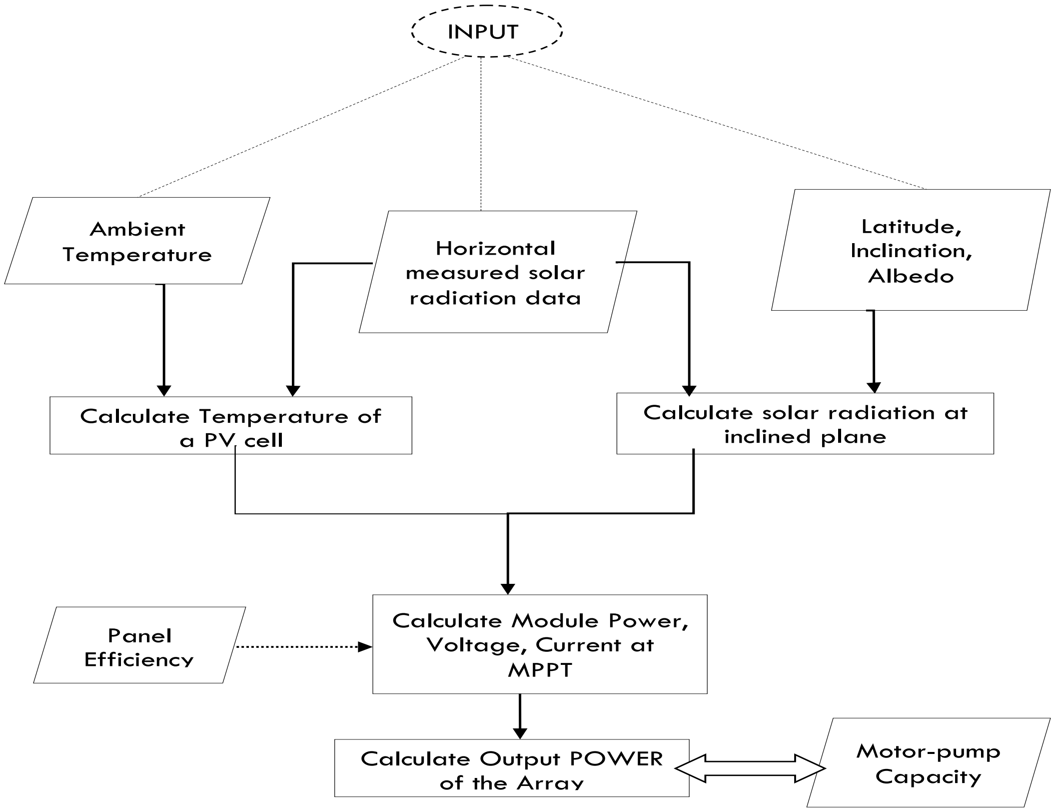

Figure 7: Flow chat diagram of solar PV energy output.

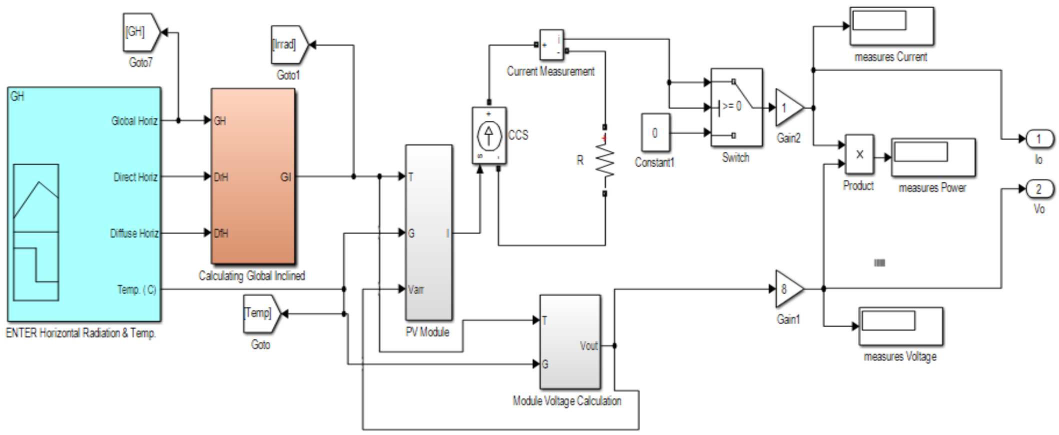

Figure 81: MATLAB block representation of PV array model with input and output data.

Inverter Model

The results of Equation (9) were used to calculate power output of inverter. The following formula was used,

$$P_{out-AC} = \eta_{inv} P_{in-DC} \tag{18}$$

where, similar to Josue and Mushi (2022), the $P_{out\text{-}AC}$ is the power output from the inverter supplied to the load; the inverter input power (from the solar PV array) being $P_{in\text{-}DC}$. The inverter works at an efficiency of η_{inv} which for this case is 85%. The MATLAB simulation block representation of inverter model with input and output data is as shown in Figure 9.

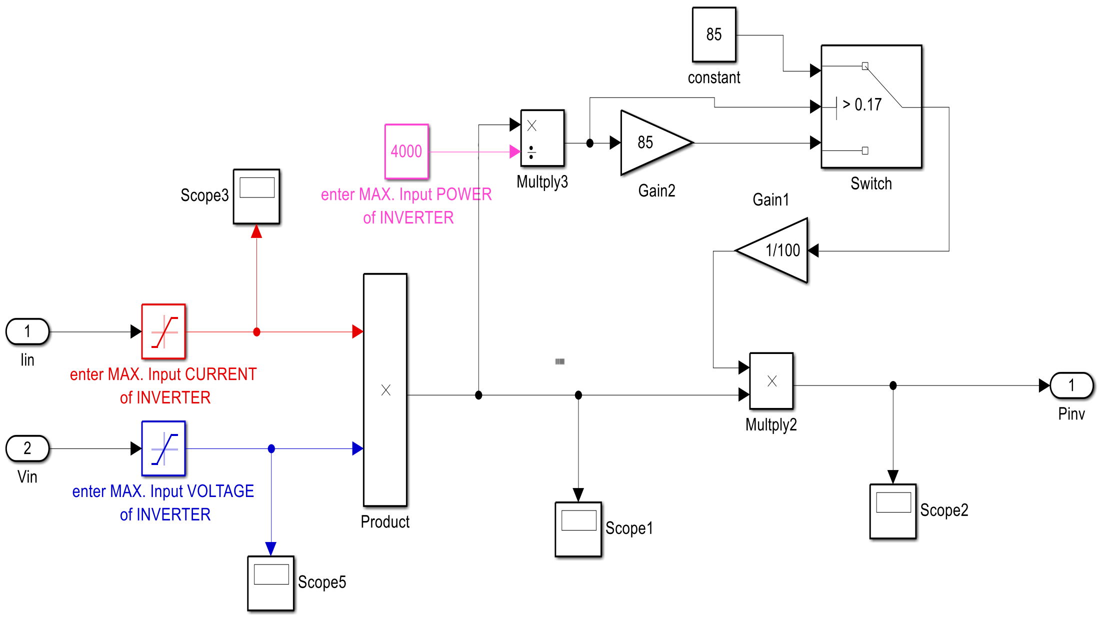

Figure 92: MATLAB block representation of inverter model with input and output data.

Motor Pump Model

Pump size is determined by considering total dynamic head, flow rate and pump efficiency as represented in Equation (19). Moreover, motor size (electric power) is determined by pump/shaft size (which is mechanical power) and motor efficiency, refer Equation (20). In simplicity, motor-pump size can just be determined by considering manufacturer's pump selection curves (Nguyen et al., 2015). Then, formula for determining hydraulic power (P_h, kW) is indicated by Equation (19).

$$P_h = \rho g H Q \tag{19}$$

For calculation purposes, pump and motor efficiencies are incorporated as there is no machine with 100%. To be specific motor pump power can be expressed as shown in the following.

$$P_m = \frac{P_s}{\eta_m} = \frac{\rho g H Q}{3600\eta_p \eta_m (1000)} \tag{20}$$

Where P_s is the pump/shaft power (kW), P_m is the motor power (kW); Q is the pump design capacity (m³/h); H is the total pumping head (m), this is also equal to $h+\Delta H$ is the hydraulic losses; g is the gravitation force (m/s^2) equaling to 9.81; ρ is the density of water (1000 kg/m^3). The pump efficiency is η_p (60-70%), motor efficiency is η_p (80-90%). Equation (20) is used to estimate size of the motor by having input values like density of water.

Since motor power is the same as the inverter output power, the formula employed to calculate water discharges becomes the following.

$$Q = \frac{\eta_m \eta_p P_{out-AC} (3600)(1000)}{\rho g H} \tag{21}$$

Figure 10 and 11 present a mathematical flow chat diagram and MATLAB simulation blocks of motor pump subsystems. They indicate step by step procedures involved during computation of motor output power.

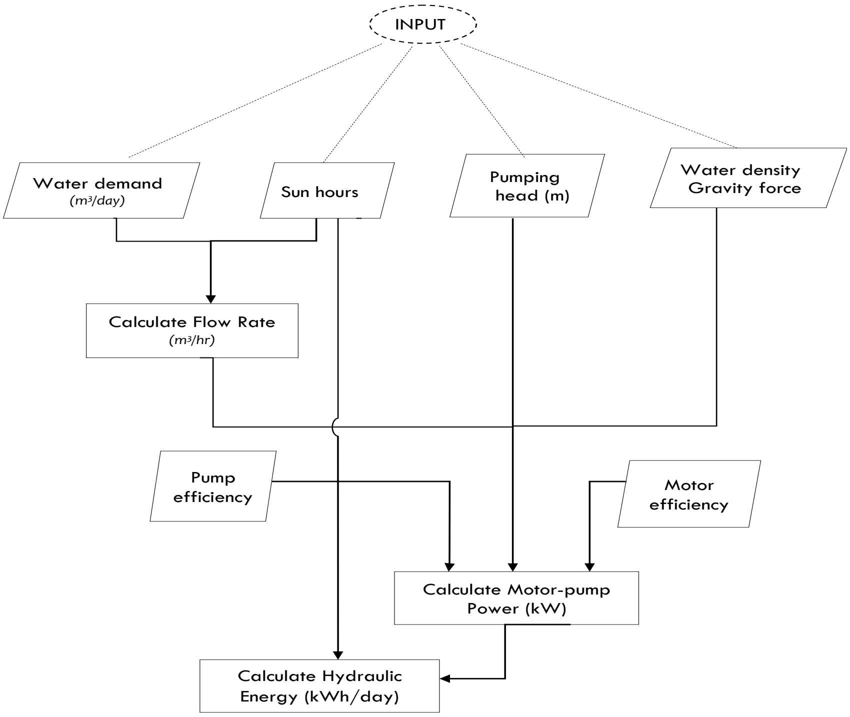

Figure 103: Motor pump subsystem mathematical flow chat diagram.

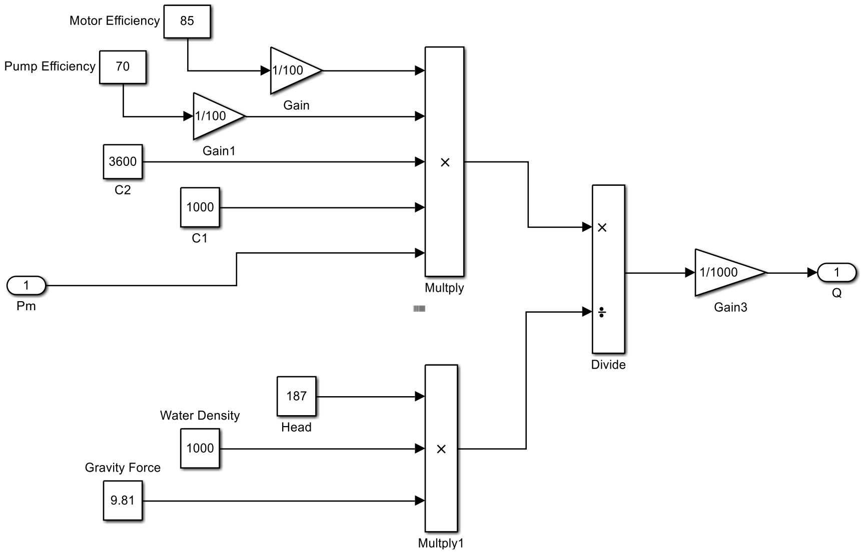

Figure 114: MATLAB block representation of motor pump model with input and output data.

Model Validation

The photovoltaic solar water pumping system model developed was validated by taking actual operating data of the system installed at Kikombo, Dodoma. Then they were compared with the simulated results. The aim of validating is to ensure if the developed models of PV array, inverter and motor pump are operating close to the expected real situation in the field. Validation was done by comparing the modelled data output result to measured data result. The result of each model was represented by graphs, showing relationship between the measured data and simulated ones. From the graph demonstration, validation measures can be concluded on whether the models are viable or not.

RESULTS AND DISCUSSIONS

Various graphs presented in Figure 12 showing simulation results of a photovoltaic solar water pumping system. A comparison between the global solar radiation measured at horizontal and inclined plane is presented too. The graph presents how inclined PV modules maximize the amount of solar radiation falling on them. For the simulated duration of time, higher values of solar radiation at inclined planes can be obtained. Moreover, PV output power, motor power, the water flow rate and the PV module temperatures are presented for three consecutive months.

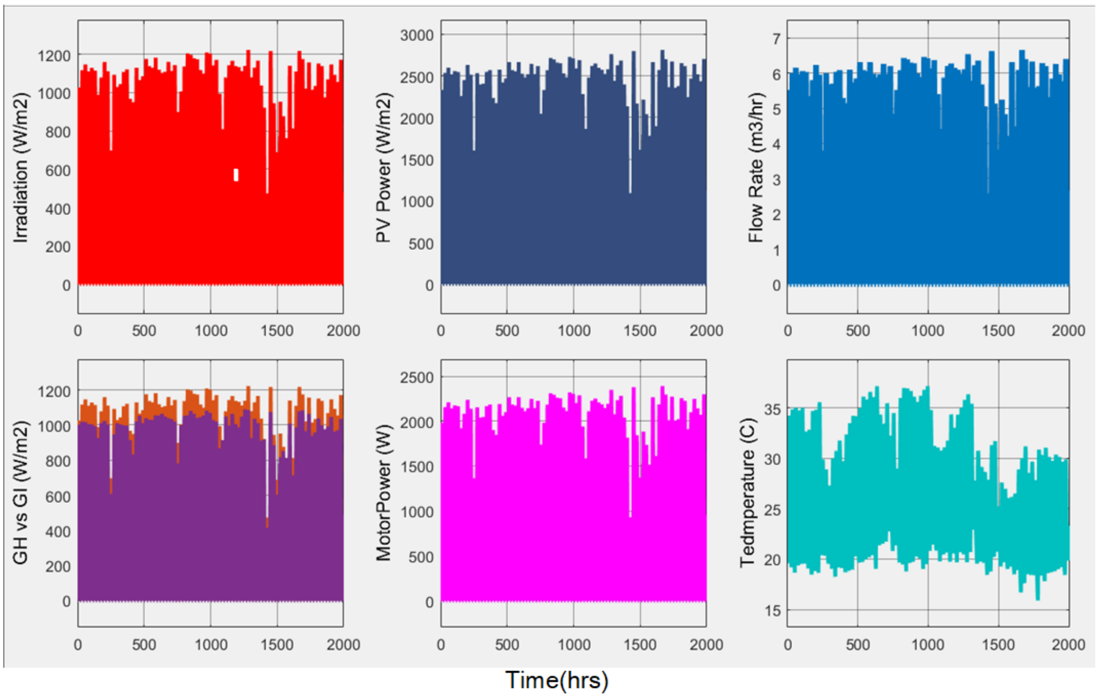

Figure 12: Various output graphs of a PVWPS as simulated in MATLAB for solar radiation, temperature, GH Vs GI, PV power, motor power and water flow rate.

Photovoltaic Solar Water Pumping Model Validation

The model was developed using MATLAB software and validated through real field measurement data. Output current and voltage from the PV model, the output (AC) power of the inverter and the flow rate were compared to those of measured at site. Both measured and simulated data were compared for analysis using MATLAB software, based on measuring the following:

a) Output current, voltage and power (DC) of the PV modules;
b) Output power (AC) of the inverter; and
c) Water flow rate of the motor pump system.

Comparison Between Simulated and Measured Values

Simulation results indicate that the current, voltage and power values from the solar panels (8 pcs rated at 315 W) has minor deviation as compared to measured data at site. The following errors were noted: 5.09% for power, 3.83% for current and 1.31% for voltage, and are illustrated in Figures 13, 14 & 15. Likewise, for the case of the inverter model (4 kW) a minor deviation of 0.0686 was observed as illustrated in Figure 16 b. The error was observed with the flow-rate of the pump with a value of 0.0406 as illustrated in Figure 19.

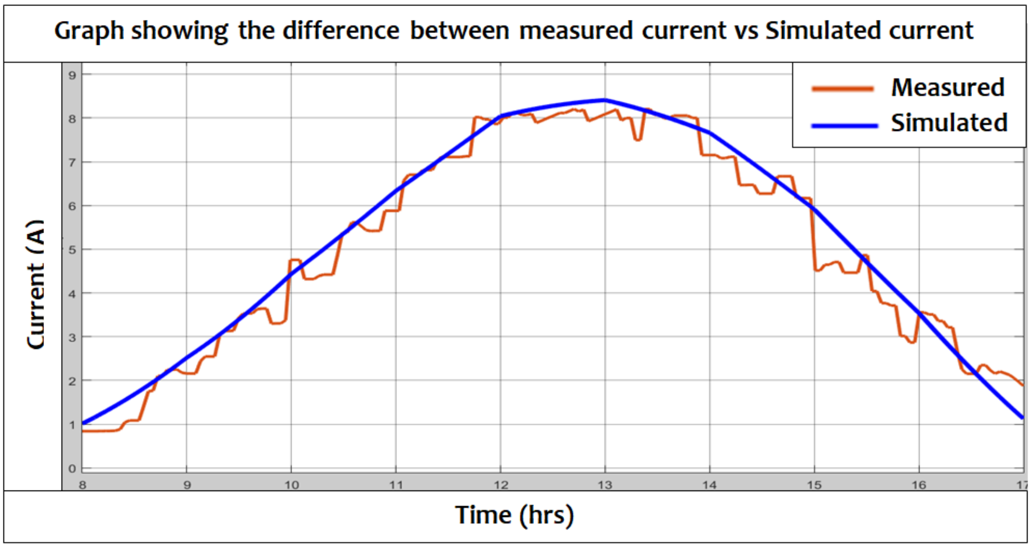

Figure 13: Comparison between measured PV current and simulated current.

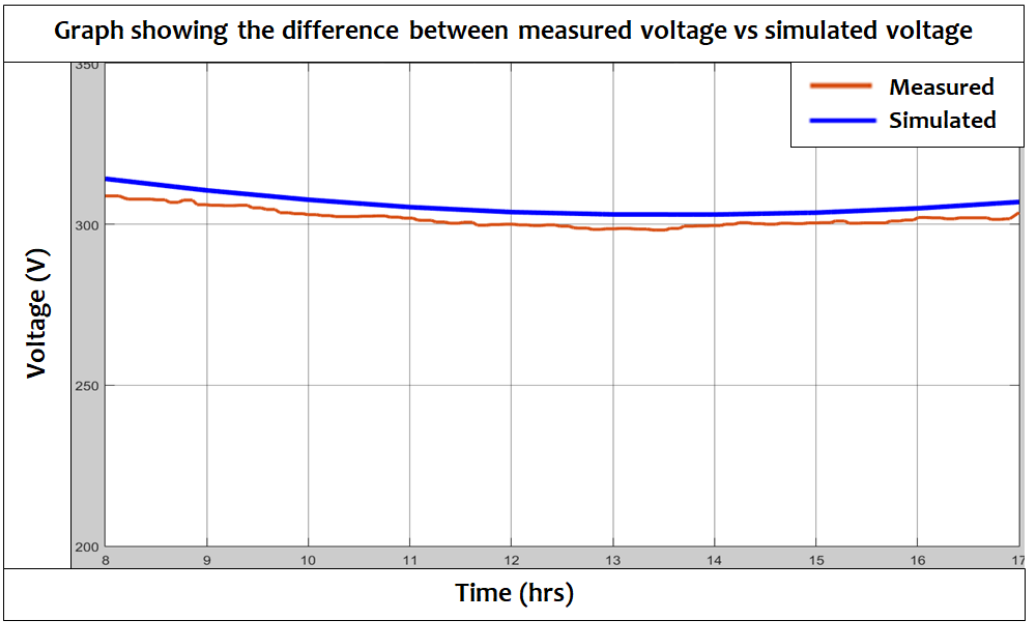

Figure 14: Comparison between measured PV voltage and simulated voltage.

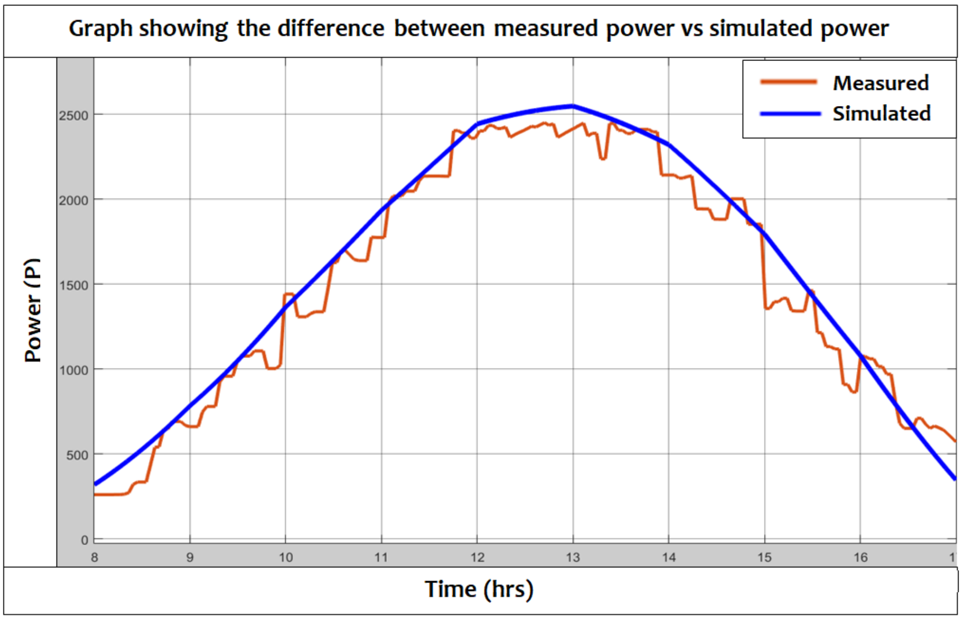

Figure 15: Comparison between measured PV power and simulated power.

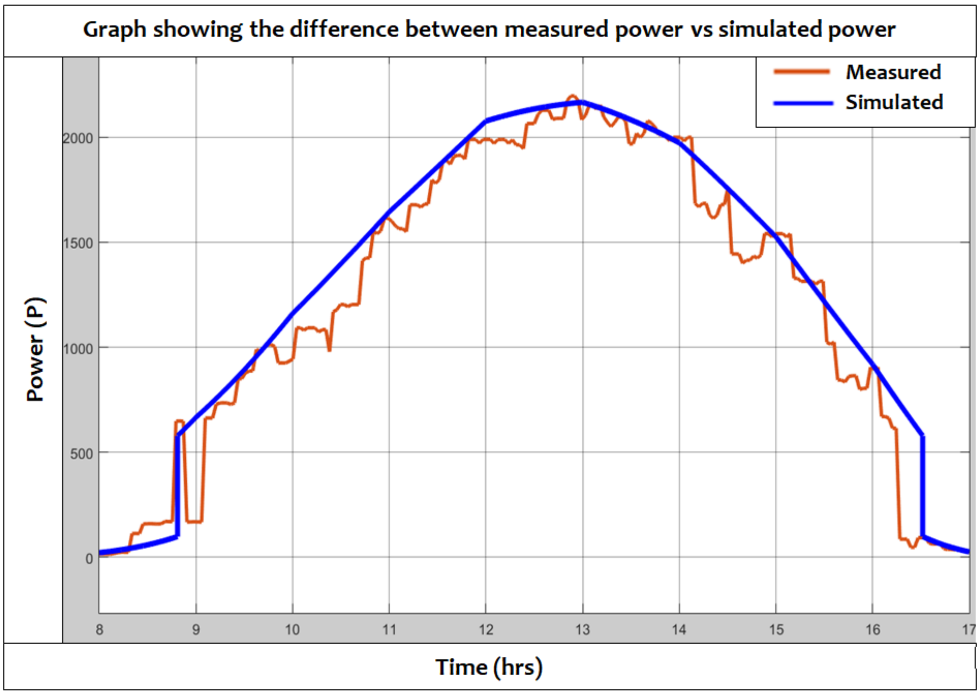

Figure 18: Comparison between measured inverter power and simulated power.

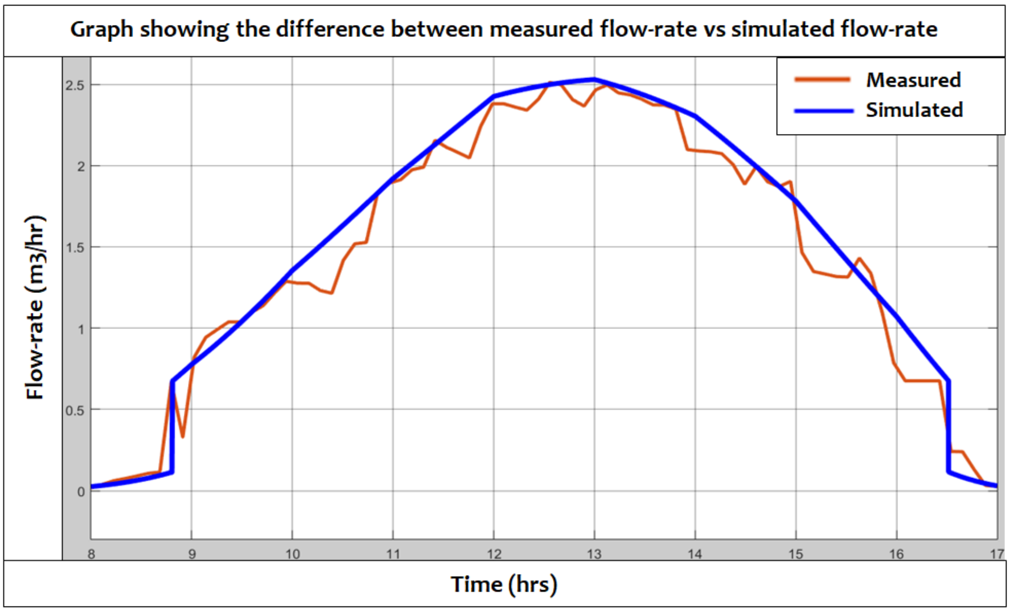

Figure 19: Comparison between measured motor-pump flow rate and simulated flow rate.

Energy and Water Flow-Rate Analysis

Electrical energy produced over a period of 9 hrs from 8:00 to 17:00 hrs from simulation result is 14.57 kWh/day and does deliver water of about 13.91 m^3. On comparing with measured data, the electricity used was 13.83 kWh/day and delivered 13.11 m^3 of water over for the same period of time. Minor error can be observed of 5.08% and 5.215% for electricity energy and water-discharge respectively.

Technical Analysis of Kikombo Solar Water Project

Since the main problem of Kikombo solar water project presented in this paper is unsatisfactory amount of water to satisfy population demand, analysis was done using the developed model to estimate which parameters should be corrected to meet requirements. Since water flow is directly proportional to PV output power, the PV output power was increased until the required water flow demand was attained. Consider Figure 20 showing how flowrate relates to solar PV power.

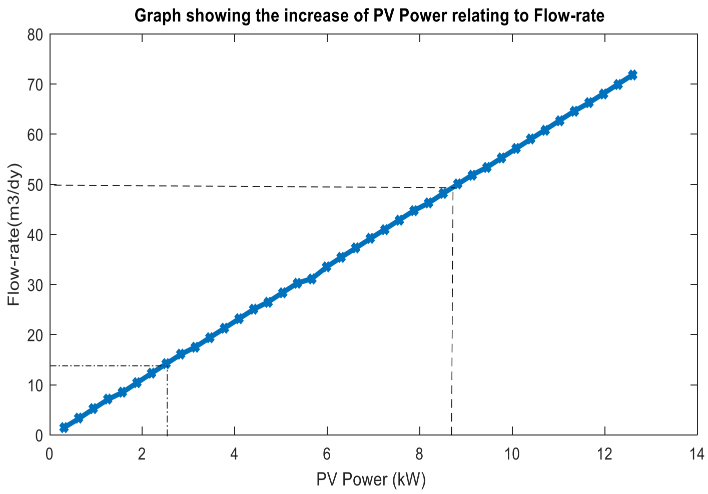

Figure 20: Relationship between PV-power (kW) against flow-rate (m^3/hr).

Two different scenarios were conducted to come up with the best option for rectifying Kikombo solar water project. The first scenario is to maintaining the existing PV panel power at 2.5 kW. From Figure 20, remarkable observation is drawn in a way that, the existing PV panel of 8 pcs, each rated 315 W is generating 2.5 kW (at peak sun), with pump capacity 2.1 kW to give an output of 14.21 m^3/day of water. This amount is less than the required demand of 50 m^3/day. This calls an attention to increase the size of PV panels and pump.

The second scenario is to increase both sizes of PV modules and pump. It can be shown from Figure 20, in order to meet the demand of 50 m^3 per day; PV modules output power should be increased to 8.82 kW with the corresponding size of motor-pump of 7.35 kW. Odeh et al. (2006); Badoud et al. (2013); and Chilundo et al. (2018) reported that, the allowable error for any developed model should be below or equal to 5%. Since such criterion is matched in this study, the proposed model can be adopted at any place to estimate the sizes of the solar water pumping system to be installed.

CONCLUSION

This paper presents a photovoltaic solar water pumping model as a tool which can be used by engineers in designing solar water pumping system. The background of this was the under design of the Kikombo solar water pumping project which does not meet the required daily demand. The proposed tool was validated in the field and presented some minor errors of less than 5%. Moreover, this paper gives a solution to the poor designed Kikombo solar water pumping project. In order to meet the required demand of 50 m^3/day, the PV solar module and pump capacities should be increased from 2.5 kW to 8.82 kW and from 2.1 kW to 7.35 kW respectively.

REFERENCES

AfDB_Group. (2015). *Tanzania Country Profile, Trade in the East African Community: Facilitation Measures and Potential Benefits*, 155–171.

Aliyu, M., Hassan, G., Said, S.A., Siddiqui, M.U., Alawami, A.T. and Elamin, I.M. (2018). A review of solar-powered water pumping systems. *Renewable and Sustainable Energy Reviews*, **87**: 61–76. https://doi.org/10.1016/j.rser.2018.02.010.

Ayeng'o, S.P. (2019). *Optimization of Number of PV Cells Connected in Series for a Direct-Coupled PV System With Lead-Acid and Lithium-Ion Batteries*. PhD Thesis, Aachener Beiträge des ISEA Band 122. https://doi.org/10.18154/RWTH-2019-01843.

Badoud, A.E., Khemliche, M., Bouamama, B.O., Bacha, S. and Villa, L.F.L. (2013). Bond graph modeling and optimization of photovoltaic pumping system: Simulation and experimental results. *Simulation Modelling Practice and Theory*, **36**: 84–103. https://doi.org/10.1016/j.simpat.2013.05.001.

Benghanem, M., Daffallah, K.O., Joraid, A.A., Alamri, S.N. and Jaber A. (2013). Performances of solar water pumping system using helical pump for a deep well: A case study for Madinah, Saudi Arabia. *Energy Conversion and Management*, **65**: 50–56. https://doi.org/10.1016/j.enconman.2012.08.013.

Bishoge, O.K., Zhang, L. and Mushi, W.G. (2018). The Potential Renewable Energy for Sustainable Development in Tanzania: A Review. *Clean Technologies*, **1**(1): 70–88. https://doi.org/10.3390/cleantechnol1010006.

Bolaji, B.O. and Adu, M.R. (2007). Design Methodology for Photovoltaic Pumping System Suitable For Rural Application in Nigeria. *ASSET Series B (2007)*, **6**(2): 120-130.

Chilundo, R.J., Mahanjane, U.S. and Neves, D. (2018). Design and Performance of Photovoltaic Water Pumping Systems: Comprehensive Review towards a Renewable Strategy for Mozambique. *Journal of Power and Energy Engineering*,

6(7), 32–63. https://doi.org/10.4236/jpee.2018.67003.

Campana, P.E. Li, H. and Yan, J. (2013). Dynamic modelling of a PV pumping system with special consideration on water demand. *Applied Energy*, **112**: 635-645. https://doi.org/10.1016/j.apenergy.2012.12.073.

Fungo, L.J., Mushi, A.T. and Msigwa, C.J. (2021). Grid Connected PV-Wind Energy System for Luxmanda Village in Tanzania. *The Third Annual Conference on Research and Inclusive Development*, 86.

Josue, N.O. and Mushi, A.T. (2022). Renewable Energy Microgrids to Improve Electrification Rate in Democratic Republic of Congo: Case of Hydro, Municipal Waste and Solar. *Tanzania Journal of Engineering and Technology*, **41** (2): 82-97. https://doi.org/10.52339/tjet.v41i2.781.

Juma, M.I., Mwinyiwiwa, B.M.M., Msigwa, C.J. and Mushi, A.T. (2021). Design of a Hybrid Energy System with Energy Storage for Standalone DC Microgrid Application. *Energies*, **14**(18): 5994. https://doi.org/10.3390/en14185994.

Justo, J.J. and Mushi, A.T. (2020). Performance Analysis of Renewable Energy Resources in Rural Areas: A Case Study of Solar Energy. *Tanzania Journal of Engineering and Technology*, **39**(1): 1-12. https://doi.org/10.52339/tjet.v39i1.514

Karafil, A., Ozbay, H. and Kesler, M. (2016). Temperature and Solar Radiation Effects on Photovoltaic Panel Power. *Journal of New Results in Science*, **5**(12): 48–58.

Ganesh, S., Bhende, C. and Mishra, S. (2011). Photovoltaic based water pumping system. *Proceedings of 2011 International Conference on Energy, Automation and Signal, ICEAS*. 448–451. http://dx.doi.org/10.1109/ICEAS.2011.6147148.

Marcel, E.T., Mutale, J. and Mushi, A.T. (2021). Optimal Design of Hybrid Renewable Energy for Tanzania Rural Communities. *Tanzania Journal of Science (TJS)*, **47**(5): 1716–1727. https://doi.org/10.4314/tjs.v47i5.19.

Masters, G.M. (2013) *Renewable and Efficient Electric Power Systems*. Wiley Interscience.

Minja, M.N. and Mushi, A.T. (2023). Design of International Airport Hybrid Renewable Energy System. *Tanzania Journal of Engineering and Technology*, **42**(1): 46-57. https://doi.org/10.52339/tjet.v42i1.887.

Nguyen, X.H. and Nguyen, M.P. (2015). Mathematical modeling of photovoltaic cell/module/arrays with tags in Matlab/Simulink. *Environmental Systems Research*, **4**(1): https://doi.org/10.1186/s40068-015-0047-9.

Odeh, I., Yohanis, Y.G. and Norton, B. (2006). Influence of pumping head , insolation and PV array size on PV water pumping system performance. **80**(1): 51–64. https://doi.org/10.1016/j.solener.2005.07.009.

Sarhan, W.M., Alkhateeb, A.N., Omran, K.D. and Hussein, F.H. (2006). Effect of temperature on the efficiency of the thermal cell. *Asian Journal of Chemistry*, **18**(2): 982–990.

Moharram, K.A., Abd-Elhady, M.S., Kandil, H.A. and El-Sherif, H. (2013). Enhancing the performance of photovoltaic panels by water cooling. *Ain Shams Engineering Journal*, **4**(4): 869-877. https://doi.org/10.1016/j.asej.2013.03.005.

Tian, H., Mancilla-David, F., Ellis, K., Jenkins, P. and Muljadi, E. (2012). A Detailed Performance Model for Photovoltaic Systems. *Preprint NREL/JA-5500-54601*, Accessed on https://www.nrel.gov/docs/fy12osti/54601.pdf on 31st October 2023.

World_Bank. (2020). *Global Water Security and Sanitation Partnership (GWSP) - Annual Report 2020*.